

XII INTERNATIONAL SYMPOSIUM ON RADIATION FROM RELATIVISTIC ELECTRONS
IN PERIODIC STRUCTURES — RREPS-17
18–22 SEPTEMBER, 2017
DESY, HAMBURG, GERMANY

Spectral structure of a polycapillary lens shaped X-ray beam

A.S. Gogolev,^{a,1} N.A. Filatov,^a S.R. Uglov,^a D. Hampai^b and S.B. Dabagov^{b,c,d}

^a*Tomsk Polytechnic University,*

Lenin Avenue 30, Tomsk, 634050 Russia

^b*INFN Laboratori Nazionali di Frascati,*

Via E. Fermi 40, Frascati, 00044 Italy

^c*NR Nuclear University MEPhI,*

Kashirskoye Shosse 31, Moscow, 115409 Russia

^d*RAS PN Lebedev Phys Inst,*

Leninsky pr. 53, Moscow, 119991 Russia

E-mail: gogolev@tpu.ru

ABSTRACT: Polycapillary X-ray optics is widely used in X-ray analysis techniques to create a small secondary source, for instance, or to deliver X-rays to the point of interest with minimum intensity losses [1]. The main characteristics of the analytical devices on its base are the size and divergence of the focused or translated beam. In this work, we used the photon-counting pixel detector ModuPIX to study the parameters for polycapillary focused X-ray tube radiation as well as the energy and spatial dependences of radiation at the focus. We have characterized the high-speed spectral camera ModuPIX, which is a single Timepix device with a fast parallel readout allowing up to 850 frames per second with 256×256 pixels and a $55 \mu\text{m}$ pitch defined by the frame frequency. By means of the silicon monochromator the energy response function is measured in clustering mode by the energy scan over total X-ray tube spectrum.

KEYWORDS: Inspection with x-rays; Computerized Tomography (CT) and Computed Radiography (CR); Detector alignment and calibration methods (lasers, sources, particle-beams); Detector control systems (detector and experiment monitoring and slow-control systems, architecture, hardware, algorithms, databases)

¹Corresponding author.

Contents

1	Introduction	1
2	Equipment and method	1
2.1	Experimental setup	2
2.2	ModuPIX characterization	2
2.3	Polycapillary lens characterization	3
3	Discussion and conclusion	5

1 Introduction

Polycapillary X-ray optics has been widely used in X-ray analysis techniques [1–4] providing advanced beam characteristics such as the size and the divergence of transmitted beam requested by newly designed analytical instruments. The parameters of the polycapillary focused beam vary with the radiation energy and the distance from the exit of polycapillary lens as well [1, 4]. This fact should be taken into account to optimize the performance of X-ray imaging systems based on the use of polycapillary X-ray optics in combination with multi-energy (spectral) methods by means of photon-counting detectors [6, 7]. Present matrix detectors utilizing the photon-counting principle open new prospects for micro-computed tomography (μ CT) [8]. The main advantage of these detectors is their ability to set the energy threshold that allows “color imaging” in the X-ray region. The energy dependence for absorption might be used to recognize the component composition of an object [9] that is particularly important for medical/biomedical imaging as well as industrial applications. In addition, polycapillary X-ray optics might be considered as an alternative method based on coherence when a focusing lens in combination with a pinhole applied to conventional X-ray tube is utilized for phase-contrast imaging [6].

In this work we present our recent studies on focus size of polycapillary optics and on divergence dependences for X-ray tube radiation that have been measured by the high-speed spectral camera ModuPIX [10] in photon-counting mode.

2 Equipment and method

We experimentally investigated the spectral structure of a focused X-ray beam by polycapillary lens using a laboratory bench-top. In this section, parameters of the setup, data acquisition, and processing are discussed in detail.

2.1 Experimental setup

The experimental setup was based on optical stages that allow high-precision multi-axial freedom. Figure 1 presents a picture of the experimental laboratory bench-top. As a source we use a BSV-29 silver-anode X-ray tube produced by the Svetlana-X-Ray company [11]. The main characteristics of the tube are defined by the voltage maximum HV of 60 kV, the current of 10 mA, and the source focus size of 0.4×0.8 mm.

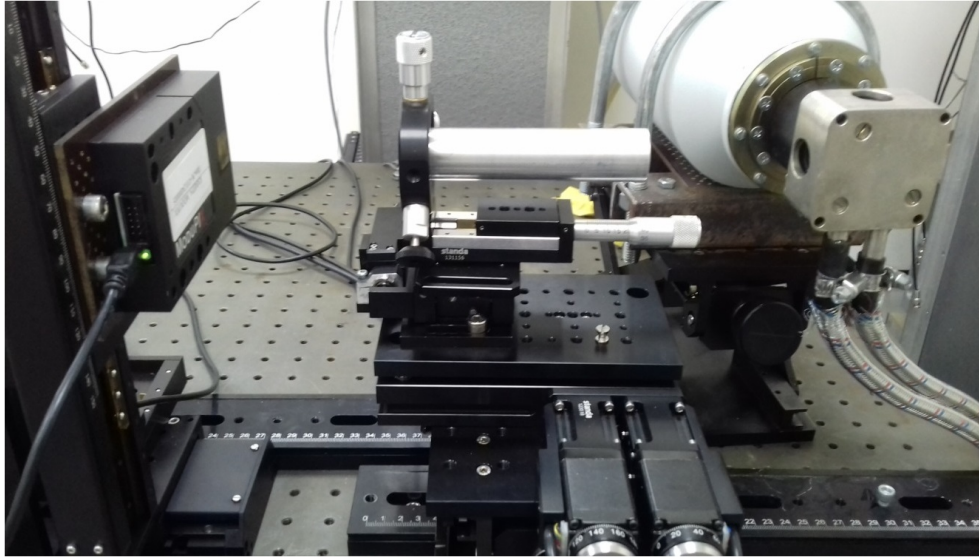


Figure 1. The experimental setup.

The acquisition system was equipped with the ModuPIX photon-counting detector based on a single Timepix chip (256×256 pixels, $55 \mu\text{m}$ pixel size) with a $675 \mu\text{m}$ thick silicon sensor [10]. The ModuPIX fast parallel readout allows collecting up to 850 frames per second in several modes. The measurements were performed in clustering mode permitting on-line identification of the photons energies but with a lower energy resolution than in a threshold scan mode [12, 13].

The main object studied was a polycapillary lens (full lens) manufactured by the technological unit X-Channel of Xlab Frascati LNF INFN [14]. According to the data sheet, the lens characteristics are as follows: the entrance focus distance $f_1 = 51.5$ mm, the exit focus distance $f_2 = 47.5$ mm, the length $L = 113$ mm, the entrance end diameter $D_{\text{in}} = 4.5$ mm, the exit end diameter $D_{\text{out}} = 3.8$ mm, the maximum diameter $D_{\text{max}} = 6.4$ mm, and the capture angle (the aperture) of 5.0° .

2.2 ModuPIX characterization

The detector was calibrated at the laboratory bench-top using a two-axis Si (400) crystalline monochromator (figure 2). The angular scan was performed in the symmetric Laue geometry, revealing, for example, the diffraction line collected from several hundred frames (figure 2 inset).

The spectroscopic properties of the photon-counting detectors are typically degenerated by the charge-sharing phenomenon [12, 13]. In order to minimize this effect, we perform the measurements in a clustering (charge-summing) mode when the charge is collected from several neighboring pixels.

In our actual measurements we have used the cluster of 2×2 pixels with optimized time exposition to avoid signal overlapping.

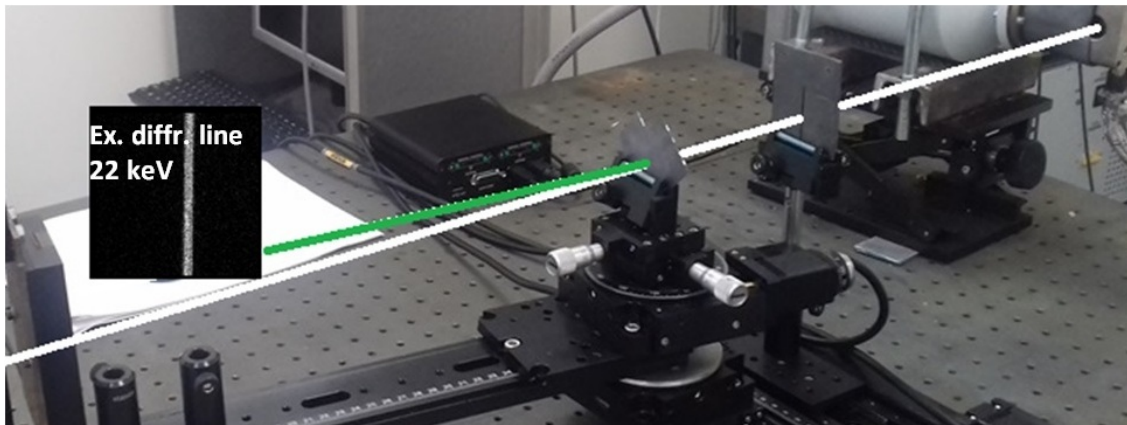


Figure 2. Si crystal monochromator for calibrating the ModuPIX. The inset shows the diffraction line, collected from several hundred frames.

Figure 3 (left) demonstrates the measured detector responses as functions of X-ray energy at a 10 keV threshold (THL) and 200 V bias level. They all correspond to a typical response for ModuPIX detectors in a clustering mode. As expected, the linewidth grows with the radiation energy increase, keeping the resolution in the whole energy range within 13% of its value.

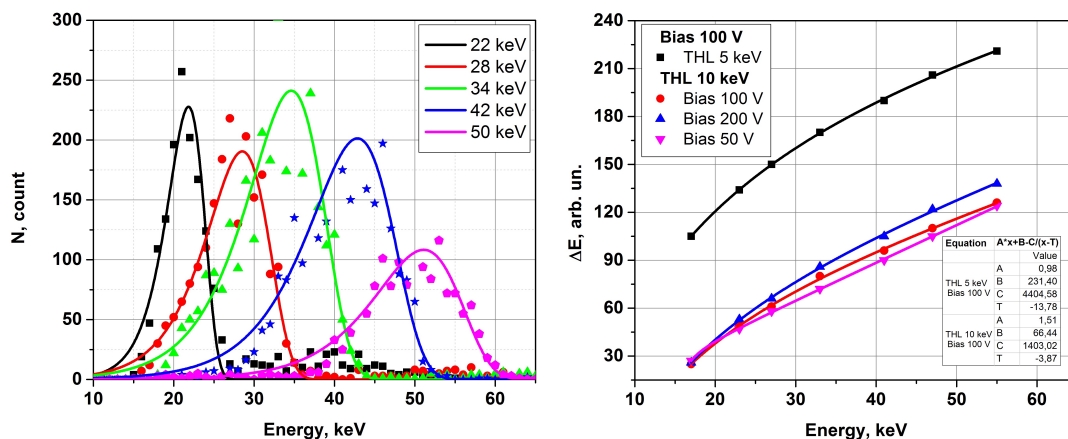


Figure 3. Measured detector response (left) and calibration curves (right).

Figure 3 (right) shows corresponding dependences of the deposition energy ΔE vs diffracted photon energy in the detector ADC channels for different threshold and bias levels. The energy of diffracted photon defined by Braggs law is calibrated by the energy-dispersive spectrometer with 300 eV energy resolution. In the following we have presented the measured data at 10 keV threshold and 200 V bias level, which were determined as optimal.

2.3 Polycapillary lens characterization

In order to apply the optics at our experimental desktop facility the polycapillary lens was investigated. The aim of the study was in measuring the virtual focus size as well as the divergence for

a wide spectral X-ray range. After adjusting the system in general, the focal distance f_2 was determined via scanning the radiation distribution along the optical axis. The minimum cross section of X-ray beam was registered at 47.5 mm from the exit that corresponds to the manufacturer data sheet. The lens characteristics as a function of the radiation energy were defined at four various points of the detector position: the point 1 for $f_2/2 = 23.75$ mm, the point 2 for f_2 , the point 3 for $3f_2/2$, and the point 4 for $2f_2$. Figure 4 shows the cross sections of X-ray beam at the points 2 and 4 versus X-ray energy.

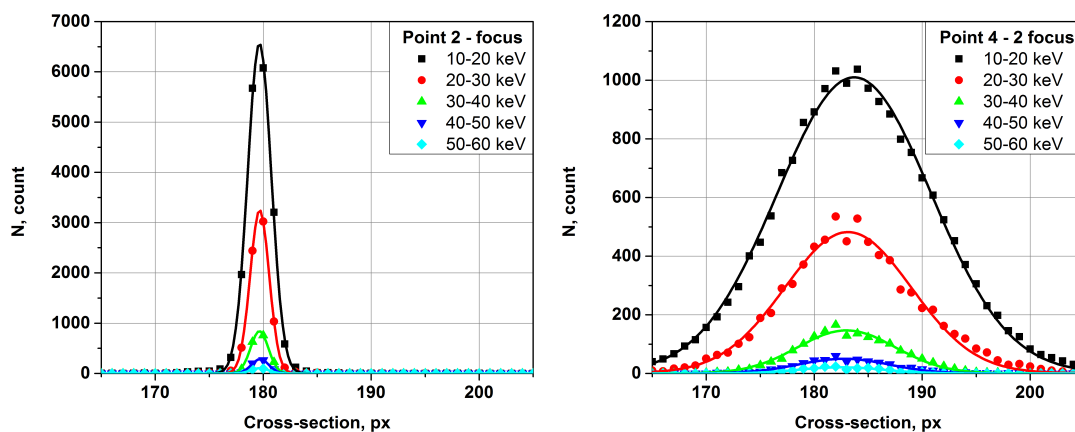


Figure 4. X-ray beam cross sections at the focus point (left) and the double-focus position (right).

Figure 5 presents the measurement results for both divergence (left) and normalized cross sections at the focus point (right). These data indicate that the size of a focal spot increases from 112 to 151 μm when the radiation energy decreases from 60 to 10 keV. The divergence increases for lower energies: for the studied lens, the values vary from 0.6° to 1.2° for bins energy of 50–60 keV and 10–20 keV, respectively.

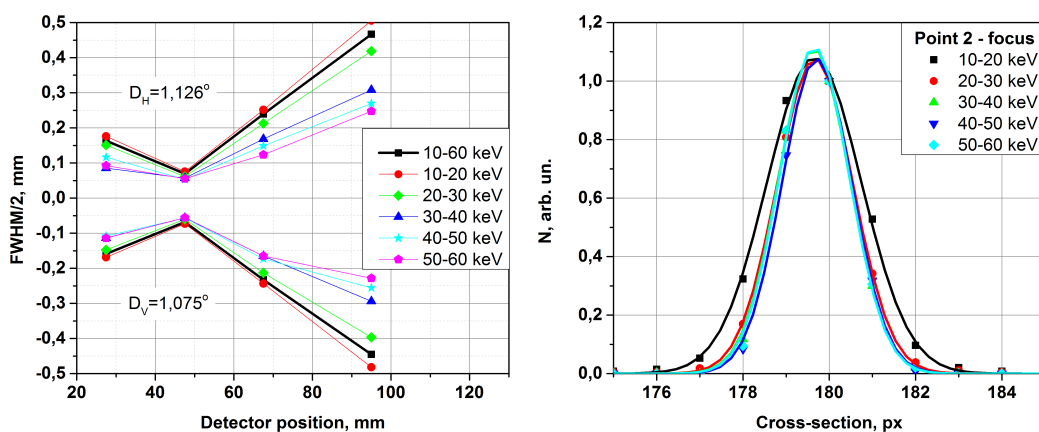


Figure 5. Measured divergence (left) and focus size (right).

In figure 5 (left), the positive area of the graph corresponds to half the horizontal cross section, and the negative half corresponds to the vertical cross section. The results indicate that radiation with energy higher than 30 keV has been also effectively focused. However, although the focus

size for energy over 30 keV does not practically change, the beam divergence distinctly decreases for higher energies. The dependence of the beam divergence on the radiation energy agrees with the results of the transmissivity studies for a single curved capillary [15]. As shown in [2], the inclination angle of the outer channels of the focusing lens determines the maximum angle of the global divergence of the radiation. At the same time, external channels are characterized by a greater bending angle (greater curvature). The transmissivity for curved capillaries depends on both the bending radius and the photon energy [15]. With the decrease of the bending radius (the increase of the curvature), the transmission of 60 keV photons for capillaries decreases faster than for 30 keV photons. It takes place because of the inversal proportionality of the angle of total external reflection to the photon energy. Thus, external channels having a smaller bending radius show a relatively lower transmissivity at higher energies.

Reducing the radiation flux from channels with a large angle of inclination to the central lens axis leads to efficient decrease in the divergence of a high-energy component of the beam.

3 Discussion and conclusion

Using a high-speed spectral camera, we have investigated the main properties of polycapillary lens focused X-ray radiation, paying main attention to the spectral and spatial dependencies of both size and divergence of radiation at the optics focus. For the first time, the coordinates and energy for each event of the beam shaped by polycapillary lens were simultaneously measured by the ModuPIX camera.

The registered data have shown the energy dependence for both size and divergence of the focused beam. This fact has to be taken into account when interpreting experimental results obtained by means of polycapillary optics. For example, polycapillary X-ray optics can be successfully used to improve the quality of CT systems based on conventional X-ray tubes. However, in order to overcome the energy dependence for beam divergence, we have to reduce the field of view.

Acknowledgments

This study was supported by the Federal Targeted Program of the Ministry of Education and Science of the Russian Federation agreement no. 14.578.21.0198 (RFMEFI57816X0198).

References

- [1] S.B. Dabagov, *Channeling of neutral particles in micro- and nanocapillaries*, *Phys. Usp.* **46** (2003) 1053.
- [2] C.A. MacDonald, *Focusing Polycapillary Optics and their Applications*, *X-Ray Opt. Instrum.* **2010** (2010) 867049.
- [3] A. Liedl et al., *X-ray micro-computed tomography and micro x-ray fluorescence mapping of synthetic emerald by using a laboratory polycapillary optics x-ray tube layout*, *X-Ray Spectrom.* **44** (2015) 201.
- [4] Y. Cherepennikov et al., *Application of polycapillary optics for dual energy spectroscopy based on a laboratory source*, *Nucl. Instrum. Meth.* **B 402** (2017) 278.

- [5] T. Sun et al., *Fine structures of divergence of polycapillary x-ray optics*, *Nucl. Instrum. Meth. B* **269** (2011) 2758.
- [6] S. Bashir, S. Tahir, C.A. MacDonald and J.C. Petrucci, *Phase imaging using focused polycapillary optics*, *Opt. Commun.* **369** (2016) 28.
- [7] J. Jakubek, *Semiconductor Pixel detectors and their applications in life sciences*, 2009 *JINST* **4** P03013.
- [8] J. Dudak, J. Zemlicka, J. Karch, Z. Hermanova, J. Kvacek and F. Krejci, *Microtomography with photon counting detectors: improving the quality of tomographic reconstruction by voxel-space oversampling*, 2017 *JINST* **12** C01060.
- [9] G. Anton et al., *Imaging theory for x-ray pixel detectors*, *Nucl. Instrum. Meth. A* **563** (2006) 116.
- [10] ADVACAM, *Modular high speed spectral camera ModuPIX*, (2017) <http://advacam.com/en/products/modupix>.
- [11] Svetlana-X-Ray, *Diffraction X-ray tubes with massive anode design*, (2017) <http://www.svetlana-x-ray.ru/production-list-eng.html?cid=12>.
- [12] M. Zuber, T. Koenig, E. Hamann, A. Cecilia, M. Fiederle and T. Baumbach, *Characterization of a 2×3 Timepix assembly with a $500 \mu\text{m}$ thick silicon sensor*, 2014 *JINST* **9** C05037.
- [13] T. Koenig et al., *Charge summing in spectroscopic x-ray detectors with high-z sensors*, *IEEE Trans. Nucl. Sci.* **60** (2013) 4713.
- [14] XLab/LNF-INFN, *X-LAB: Laboratorio di Ricerca e Sviluppo nel Settore dei Raggi X*, (2017) <http://www.lnf.infn.it/xlab/>.
- [15] L. Wang, B.K. Rath, W.M. Gibson, J.C. Kimball and C.A. MacDonald, *Performance study of polycapillary optics for hard x rays*, *J. Appl. Phys.* **80** (1996) 3628.